
Article:
Çelik, M., Maguire, J.M. orcid.org/0000-0003-0807-6467, Noble, T. et al. (2 more authors) (2023) Numerical and experimental investigation of Joule heating in a carbon fibre powder epoxy towpregging line. Composites Part A: Applied Science and Manufacturing, 164. 107285. ISSN 1359-835X

https://doi.org/10.1016/j.compositesa.2022.107285

Composites: Part A 164 (2023) 107285

Contents lists available at ScienceDirect

Composites Part A

journal homepage: www.elsevier.com/locate/compositesa

Numerical and experimental investigation of Joule heating in a carbon fibre powder epoxy towpregging line

Murat Çelik *, James M. Maguire, Thomas Noble, Colin Robert, Conchúr M. Ó Brádaigh

School of Engineering, Institute for Materials and Processes, The University of Edinburgh, Edinburgh EH9 3FB, UK

ARTICLE INFO

Keywords:
Powder epoxy
Joule heating
Towpregging
Process modelling

ABSTRACT

Powder epoxy based towpregs offer favourable processing and storage properties, thanks to the low viscosity and thermal stability of the powder epoxy. Low-cost, high-quality towpregs, which are suitable for automated fibre placement or filament winding applications, can be produced at a high production rate with an automated towpregging line. This study focuses on improving the towpregging process by analysing the heating characteristics of a towpregging line that employs Joule heating to impregnate carbon fibre tows with powder epoxy. A finite element analysis heat transfer model was developed to identify the relationship between processing parameters and heating of the carbon fibre tows. Model predictions matched well with experimental results. Using the temperature distribution predicted by the model, powder epoxy melting and sintering behaviour was investigated using semi-empirical equations. Results revealed that Joule heating provides efficient heating with very low power consumption. It was found that while it is possible to produce towpregs at high production speeds (15 m/min), slower speeds might yield more consistent quality. Using parametric studies in the model, it was shown that it is possible to increase towpregging line production rate without compromising the towpreg quality, by altering some of the key process parameters (supplied current, electrode distance etc.).

1. Introduction

The composites industry has benefited immensely from automated manufacturing methods in recent years, for instance, up to 85 % reduction in labour hours was reported by companies [1]. Methods such as automated fibre placement (AFP), which is an additive manufacturing process in essence, can produce composite parts at high rates with minimal material waste and error. Repeatability and accuracy of such systems are appealing to many industries [2].

In the AFP process, narrow-width prepreg tapes (towpreg) are laid on a mould layer by layer, and are consolidated with heat and pressure application by the AFP head. AFP applications are expected to play a major role in the future, especially if the current technology keeps up with the recent advances in Industry 4.0 [3]. In line with the progress in the AFP process, there is a growing interest in the materials that are used in AFP: towpregs (or prepreg tape) are one of the fastest-growing type of prepreg materials in the composite market [4]. Typically, towpreg manufacture is carried out using production lines, which can adopt melt-impregnation [5–9], powder slurry [10–12] or powder coating [13–20] techniques in order to impregnate the powder with the thermoplastic or thermoset matrix. Although AFP is a cost-effective process, conventional towpreg can be expensive. In order to reduce material costs while maintaining the quality, powder epoxy-based towpregs have been developed [21,22]. The towpregging line, or tapeline, developed by Robert et al. [21] impregnates carbon fibre tows with a novel powder epoxy. Powder epoxy composites do not require refrigerated storage conditions and have a long shelf life at room temperature, thanks to their chemical stability at room temperature [23]. From a processing perspective, the low viscosity of the molten powder epoxy results in good consolidation of the final part and relatively little heat generation when curing, minimising the risk of thermal runaway. Furthermore, little or no volatile organic compounds (VOCs) are released, and the excess powder can be recycled.

In the tapeline system [21], powder epoxy is deposited on the carbon fibre tow and melted by heating the tow through Joule (resistive) heating. Conductive carbon fibres heat up and act as individual heating elements when a current passes through, thus uniform and rapid heating can be achieved via Joule heating. It can be used in composite applications, particularly in the curing of composites, due to its simplicity, effectiveness, and efficiency. The power consumption of Joule heating is

* Corresponding author.
E-mail address: m.celik@ed.ac.uk (M. Çelik).

https://doi.org/10.1016/j.compositesa.2022.107285
Received 13 July 2022; Received in revised form 26 October 2022; Accepted 30 October 2022
Available online 5 November 2022

extremely low when compared to conventional heating systems, up to 80 % lower power consumption than oven heating was reported [24], while comparable mechanical performance was obtained. It was shown that even some mechanical properties can be improved by Joule heating; Sierakowski et al. [25] demonstrated that it is possible to enhance the impact resistance of the composites by applying DC for short periods. One of the most advantageous features of this technique is uniformity in the temperature, which results in a consistent degree of curing along the part. Although local thermal gradients might be observed in electrode–composite interfaces [26], a uniform temperature profile over the sample can be attained in Joule heating systems [27]. Furthermore, overall curing time is much shorter [28] since heat is generated directly in the carbon fibres. This contrasts with oven heating, where the air inside must be heated first before heat transfers to the composite part. Degrees of curing of parts heated with Joule heating can exceed oven-cured composite parts [29]. Other than curing, some practical applications are compatible with Joule heating, including self-healing [30–33] and de-icing [28,34]. Contact resistances occurring at the electrode–composite interfaces, however, create thermal gradients and therefore must be taken into account when designing heating systems.

Modelling methods are extensively used for calculating the heat generated by the Joule effect [25,33,35–38]. Calculating the temperature field through numerical models can improve mould design by visualising the thermal gradients. Furthermore, by coupling other process models, one can gain insight into different physics during the manufacturing, such as the curing or crystallisation behaviour of the material. With appropriate boundary conditions, temperature distribution during the Joule heating of composites can be calculated accurately [36]. As mentioned before, however, contact resistances must be defined carefully as they can be responsible for significant non-uniformities near electrode–composite interfaces [26]. It is possible to account for this additional heating by characterising the contact resistances. Sierakowksi et al. [25] demonstrated that the heating caused by contact resistances can be more significant than Joule heating for longer heating durations. Kwok and Hahn [33] accounted for the contact resistance heating in their model by introducing a thin, high resistance layer at the electrode/composite interface. Although their model overpredicts the temperature of the specimen greatly, it performed well in estimating the local hot spots. The authors claimed that the deviation is due to the actual resistivity of the material being different from the one used in the model. Similar deviations are common in Joule heating models [37,38], mainly caused by ill-defined material properties. Lu et al. [39] used a heat transfer model to analyse the heat losses occurring in a continuous polyacrylonitrile-carbon nanotube stabilisation system. They found out that, by utilising Joule heating, the stabilisation duration can be reduced from 2.5 h to under 1 h, with only 1 % of the power requirement of convective heating.

While the tapeline system can benefit from a heat transfer model, understanding the melting behaviour of the powder epoxy is equally important and can improve production. Melting and sintering of polymer powders have been explored both experimentally and numerically [40–44]. With an increase in temperature, powder polymer melting is followed by sintering, which is a double-stage mechanism including powder coalescence and bubble removal [43]. It is a widely discussed topic for rotational moulding and laser sintering applications [40,42], however, Maguire et al. [23] described the sintering of the powder epoxy for thick-section composite manufacturing, using a semi-empirical equation. From the towpreg manufacturing standpoint, it is vital to ensure that the state of the powder epoxy during the heating is optimal to provide a good degree of impregnation. By coupling heat transfer models to appropriate melting and sintering models, the ideal processing window for the manufacturing of towpregs can be determined.

Most of the towpregging systems include a crucial heating step in the production line, either to preheat fibres before the impregnation step or to melt the deposited matrix or removal of the solvent after the impregnation step [5–20]. Thermal models of such systems provide a better understanding of the overall process and the possibility to analyse the system in detail. [10]. Most of the aforementioned studies, however, sought to investigate the towpregging processes from an experimental point of view, and the developed thermal models are limited in capacity [10]. The authors previously identified the contact resistances in the Joule heating system of the tapeline in an experimental campaign, and through a simplified finite element analysis (FEA) model, they demonstrated that the accuracy of thermal models can be improved by accounting for contact resistances [45]. This paper aims to characterise the Joule heating process through a parametric thermal model supported by experimental data. Not only is the manufacturing process analysed by modelling beyond experimental limitations (power input, electrode distance etc.), but also the on-line melting and sintering behaviour of the powder epoxy is predicted, which is quite difficult to accomplish using experimental techniques. Thus, our study can be of interest to a broader community, in terms of experimental and modelling perspectives, considering the recent interest in towpreg/prepreg tape manufacturing processes [5–20]. Furthermore, similar modelling approaches can be used in different applications, such as well-known pultrusion [46–48], or niche applications such as double belt press lamination [49], localised in-plane thermal assist (LITA) technique [50,51] and radio-frequency (RF) heating [52].

2. Experimental

2.1. Tapeline system

A tapeline system has been developed [21] to produce low-cost, high-quality and fully consolidated (but not cured) powder epoxy-based towpregs that are compatible with AFP applications. In this system, carbon fibre tows are pulled through a series of rollers, powder epoxy is electrostatically deposited on the carbon fibre tow using a charged epoxy powder particle cloud in a semi-confined box under constant extraction. Joule heating is used to heat the carbon fibre tow and to melt the powder epoxy, and finally the produced towpreg is collected (Fig. 1). A detailed description of the system is provided in [21,22]. The main advantage of the tapeline system is that the towpreg production is automated and is monitored by various sensors (tow tension, temperature, speed etc.), allowing for high-volume production of high-quality towpregs. The towpregging line includes an active tension control system, which uses tension sensors to monitor the tension of the tow at all times and a PID-controlled magnetic brake to maintain a set tension on the tow, based on the data read from the tension sensor. Therefore, the tension of the tow remains constant throughout a production run. The advantageous processing properties of the powder epoxy include low viscosity, no VOCs, easy deposition and long storage life. By altering the operating parameters of the tapeline, different fibre volume fractions (and consequently different mechanical properties) can be achieved. Furthermore, another key advantage of the towpregging line is its versatility. With some alterations in the system, thermoplastics powders could be used for towpreg production, which would attract great interest due to their recyclability. Although for some thermoplastics, such as PEEK, the processing window between melt and degradation is very narrow, as the heating time is very short in the line, working with such materials could be achievable.

2.2. Joule heating

Joule heating is the preferred option in the tapeline system for heating the carbon fibre tows and is carried out after powder deposition, in order to melt the powder epoxy deposited on the tows. Two conductive copper roller electrodes are used to provide the electrical current, while infrared (IR) temperature sensors (OS-PC30-2M-1V, OMEGA Engineering) measure the temperature of the tows constantly (Fig. 2a). Based on the IR temperature sensor data, a PID controller

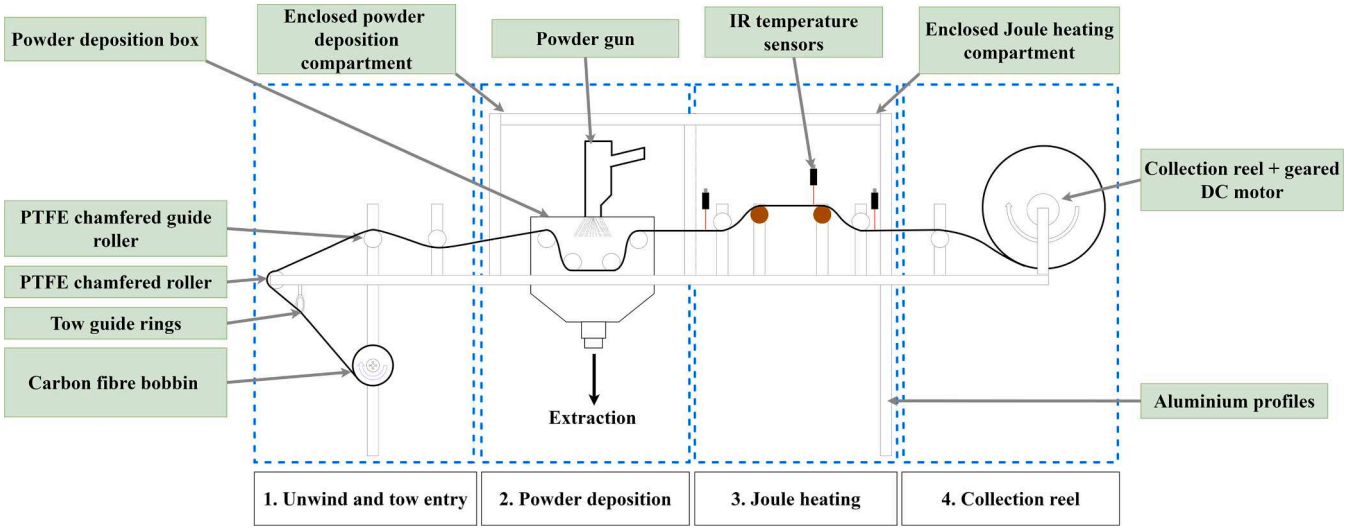

Fig. 1. Schematic of the tapeline. (For interpretation of the references to colour in this figure legend, the reader is referred to the web version of this article.)

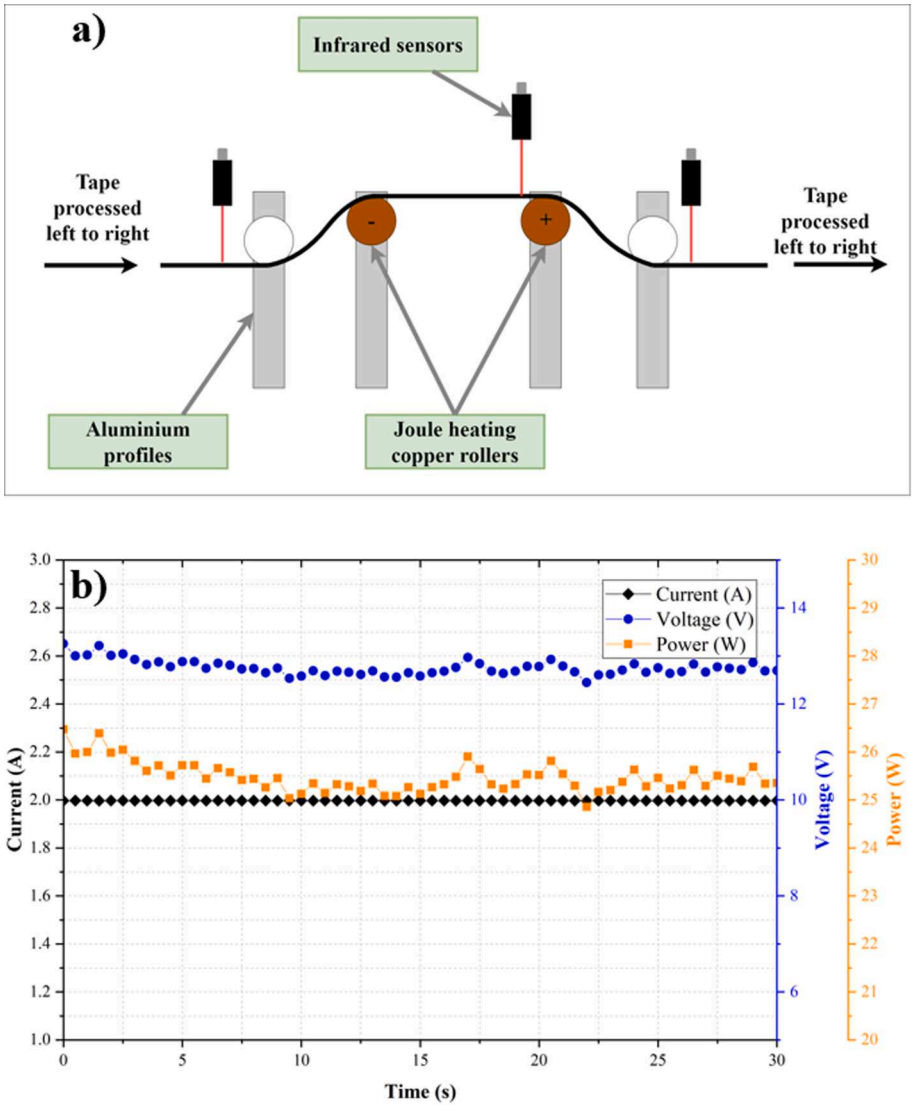

Fig. 2. **(a)** The heating section of the tapeline, **(b)** typical current, voltage and power characteristics during heating. (For interpretation of the references to colour in this figure legend, the reader is referred to the web version of this article.)

adjusts the current passing through the carbon fibre to reach the set temperature. Joule heating provides rapid heating of the carbon fibre tows (e.g. 4 s to reach 120 °C) and the power requirement is also very small, as shown in Fig. 2b (around 25 W), whereas a small curing oven typically operates at 500 W [24]. There is no further equipment required apart from the conductive rollers and PID control system, and instantaneous automated temperature control is possible with the Joule heating system. Powder epoxy and loose carbon fibre filaments can, however, build up around the conductive rollers during prolonged production runs, which can prevent the current from flowing through the fibres, resulting in disruptions in the production. To avoid powder epoxy and loose carbon fibre build up around the rollers, metal scrapers were placed underneath the copper rollers.

2.3. Materials

Toray T700S-24 K-50C (1 % sizing) carbon fibre tow and powder epoxy (PE6405, 1220 kg/m^3, supplied by FreiLacke and designed by Swiss CMT AG) were used for the towpreg production. The conductive Joule heating electrodes were made of copper. Slip-rings were fitted inside the copper electrodes to provide electric current. An infrared thermal camera (FLIR A655SC) was used to measure the temperature distribution in the carbon fibre tow.

3. Numerical modelling

3.1. Heat transfer model

Carbon fibre filaments in the tow act as heating elements when an electric current passes through, due to the Joule effect. The additional heat due to the Joule heating term can be expressed as [25]:

$$Q_{JH} = \frac{I^2}{\sigma V} \tag{1}$$

where Q_{JH} is the heat generated by the Joule heating (W/m^3), I is the current provided (A), σ is the electrical conductivity (Ω) and V is the volume of the medium (m^3). The heat equation then becomes:

$$c\rho\frac{\partial T}{\partial t} = \nabla(\mathbf{k}\nabla T) + Q_{JH} \tag{2}$$

where c is the specific heat capacity (J/kg K), ρ is the density (kg/m^3), T is the temperature (K), t is the time (s) and $\mathbf{k}$ is the thermal conductivity tensor of the carbon fibre tow (W/m K).

At the interfaces between the carbon fibre tow and the electrodes, electrical contact resistances occur due to the imperfect contact. A contact resistance heating term is used to describe this additional heating caused by the electrical contact resistances, and can be expressed as [25]:

$$Q_{CR} = \frac{I^2 R_{CR}}{A} \tag{3}$$

where Q_{CR} is the heat generated by the electrical contact resistances (W/m^2), I is the current (A), R_{CR} is the contact resistance (Ω) and A is the contact area of the interface (m^2).

In order to solve the heat equation, a 3D time-dependent finite element model was developed using COMSOL Multiphysics 5.6 software. Powder epoxy on the carbon fibre might lead to fluctuations in the temperature during the production, hence dry carbon fibre (i.e. without the powder epoxy) was considered for heat transfer modelling. The 3D domain created for the model is depicted in Fig. 3a. The model uses an Eulerian domain that accounts for the movement of the carbon fibre tow with a given production speed. Electrical contact resistances occurring at the interfaces between the metal roller electrodes and the carbon fibre tows were determined experimentally as explained in Ref [45]. The resistance of the entire system was measured for different electrode distances, and resistance values were plotted against electrode distance. Assuming the linear material resistivity, the y-intercept of the plots (zero electrode distance) were accepted as contact resistances and cable resistance of the system. Similar approaches can be found in [30,33,55]. Electrical contact resistance values obtained were applied to the contact areas at the interfaces by assigning an equivalent thin layer in the contact patches. Model parameters were given in Table 1. A mesh convergence study was carried out by increasing the element number in the domain as shown in Fig. 3b.

Due to the complex nature of the towpregging process, the following assumptions were made in the model:

- Thermal contact resistances were neglected.
- For the heat transfer model, dry carbon fibre only (i.e. no powder epoxy on the surface) was modelled, assuming powder-epoxy has no effect on the heating of the tow.
- The speed, tension and power applied were constant, while some small fluctuations of such parameters are observed during the production run.
- Material properties (heat capacity, density, thermal conductivity etc.) are constant and not a function of temperature.
- A thin resistive layer was used at the contact patches to account for electrical contact resistances.
- The carbon fibre tow is perfectly homogenous and solid, whereas in actuality, the tow characteristics change along the length due to the high number of carbon fibre filaments (24 K).
- For the melting and sintering model, the powder epoxy on the tow is perfectly distributed and it is present on every temperature node of the tow.

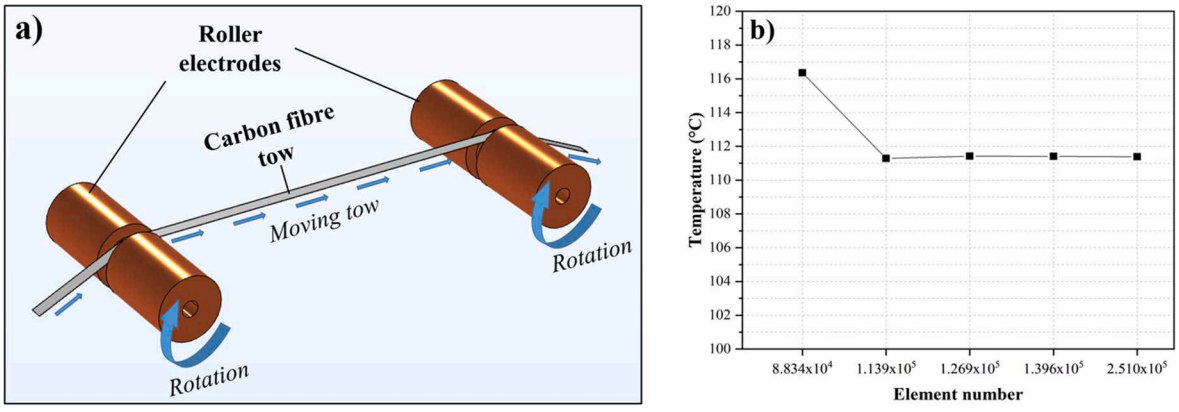

Fig. 3. (a) Computational domain and **(b)** mesh convergence plot for the model. (For interpretation of the references to colour in this figure legend, the reader is referred to the web version of this article.)

Table 1
Model parameters.

Carbon fibre tow		Copper electrodes		Electrical properties	
Density [kg/m^3] [53]	1800	Density [kg/m^3] [54]	8960	Maximum applied current [A]	2
Specific heat [J/kg.K] [53]	752	Specific heat [J/kg.K] [54]	385	Electrical contact resistance layer thickness [mm]	0.1
Thermal conductivity in the axial direction [W/m.K] [53]	9.6	Thermal conductivity [W/m.K] [54]	400	Electrical conductivity in contact resistance layer [S/m]	2.3–10
Electrical conductivity in the axial direction [S/m]	42,677	Electrical conductivity [S/m] [54]	5.99e7		
Linear velocity [m/s]	0.1083	Angular velocity [1/s]	10.83		
Width [mm]	6.35	Minimum wrap angle [°]	20		
Heated length [mm]	190	Width [mm]	98.5		
Thickness [mm]	0.2	Outer radius of the groove [mm]	10		
		Outer radius [mm]	16		
		Inner radius [mm]	4		

3.2. Melting and sintering model

Powder epoxy on the carbon fibre tows starts to melt when the temperature of the carbon fibre exceeds the melting temperature of the powder epoxy. Further temperature increments lower the viscosity, surface tension forces become dominant over the viscous forces, and the molten powder epoxy particles coalesce into a homogenous melt, a process which is defined as sintering [43]. Molten and sintered powder epoxy flows into the carbon fibre tow and upon cooling, solidifies, creating the towpreg. The sintering process creates a homogenous layer of molten powder epoxy, by merging the randomly distributed resin sites, hence the impregnation and consolidation of the resin are affected by the sintering of the powder epoxy. While it can be seen visually whether the powder epoxy melts during the production, it is important to investigate the melting and sintering behaviour further to improve production by better understanding the overall process. Through numerical modelling, process parameters can be optimised, such as the heating section length to ensure the powder is fully sintered. Thus, the heat transfer model was one-way coupled to the melting and sintering model to account for the melting behaviour of the powder epoxy.

Maguire [56] carried out thorough characterisation studies on the powder epoxy, including differential scanning calorimetry (DSC) and parallel plate rheometry (PPR) tests. By fitting Eq. (4), which was proposed by Greco and Maffezzoli [43], to the DSC data, they were able to model the melting behaviour of the powder epoxy:

$$\frac{d\theta}{dt} = k_m e^{(-k_m(T-T_m))}\left[1 + (d-1)e^{(-k_m(T-T_m))}\right]^{d/(1-d)} \tag{4}$$

where T is the temperature, k_m and d are fitting parameters, T_m is the melting point and θ is the degree of melt. The values for the fitting parameters are presented in Table 2. By coupling the heat transfer data to Eq. (4), it is possible to determine the degree of melting of the powder epoxy during the production run.

Table 2
Fitting constants for melting and sintering model, taken from Maguire [56].

Model	Fitting constants	Value
Melting model	k_m	1.83
	d	4.65
	T_m	313.58 [K]
Sintering model	χ_0	3e−5
	$C_{\chi 1}$	11.5
	$C_{\chi 2}$	24.5
	B	0.5
	χ_∞	0
	T_θ	313.58 [K]

Similar to the melting model, Maguire et al. [23] also used parallel plate rheometry (PPR) test data to relate powder sintering with thickness change, and demonstrated that sintering of the powder epoxy can be modelled with a Williams-Landel-Ferry (WLF) type of equation:

$$\frac{d\chi}{dt} = -\chi_0 \exp\left(\frac{C_{\chi 1}[T - T_\theta]}{C_{\chi 2} + T - T_\theta}\right)(\chi - \chi_\infty)^B \tag{5}$$

where χ is the degree of sintering, χ_0 is the rate constant, χ_∞ is the degree of sintering at infinity, $C_{\chi 1}$, $C_{\chi 2}$ and B are fitting constants, T is the temperature and T_θ is the melting temperature. The constants were found by fitting PPR results to Eq. (5), which are given in Table 2.

4. Numerical solution of Model, validation and discussion

4.1. Temperature distribution

The temperature distribution of the tow was obtained from the heat transfer model that was solved using COMSOL Multiphysics software. To check the validity of the model, thermal camera images of the Joule heating system were used. The model findings were compared to the average temperature distribution of the tow acquired experimentally by the thermal camera. Model predictions for voltage, heat generation and temperature distribution for 2 A current, 20 N tension and 6.5 m/min production speed are presented in Fig. 4, as well as the thermal camera image of the carbon fibre tow during the heating. Note that due to the reflective surfaces of the roller electrodes, they are not visible in the thermal camera images. The agreement between the model results and the experimental data is qualitatively good, however, a temperature gradient across the width of the tow was observed from the thermal camera images. Furthermore, the model predicts a lower temperature at the entry region to the heating section. These differences are most likely due to the higher temperatures caused by the higher tension in the middle section of the tape. Higher tension in the centre of the tape improves contact between fibres within the tow and also between the fibres and the copper rollers. Consequently, this results in a local drop of electrical resistance and more current passes in the middle of the tow than the sides; as the current prefers the least resistant path. Hence, temperature increases locally, and temperature gradients are formed across the width.

The current supplied to the heating system changes the maximum temperature reached in the carbon fibre tow. Fig. 5 compares the average experimental and model prediction temperatures across the width of the tow, at the hottest region of the tow, for different supplied currents. A good agreement between the model and experimental values is observed at the 0.5 and 1 A currents. The model underpredicts the average temperature at higher current values, however, due to the aforementioned tension inconsistency across the width of the tow. The predicted average temperature by the model at 1.5 and 2 A is ~ 75 °C and ~ 111 °C, respectively, while the thermal camera measures the temperature at these currents as ~ 85 °C and ~ 120 °C. The difference between the actual average temperature and model prediction of

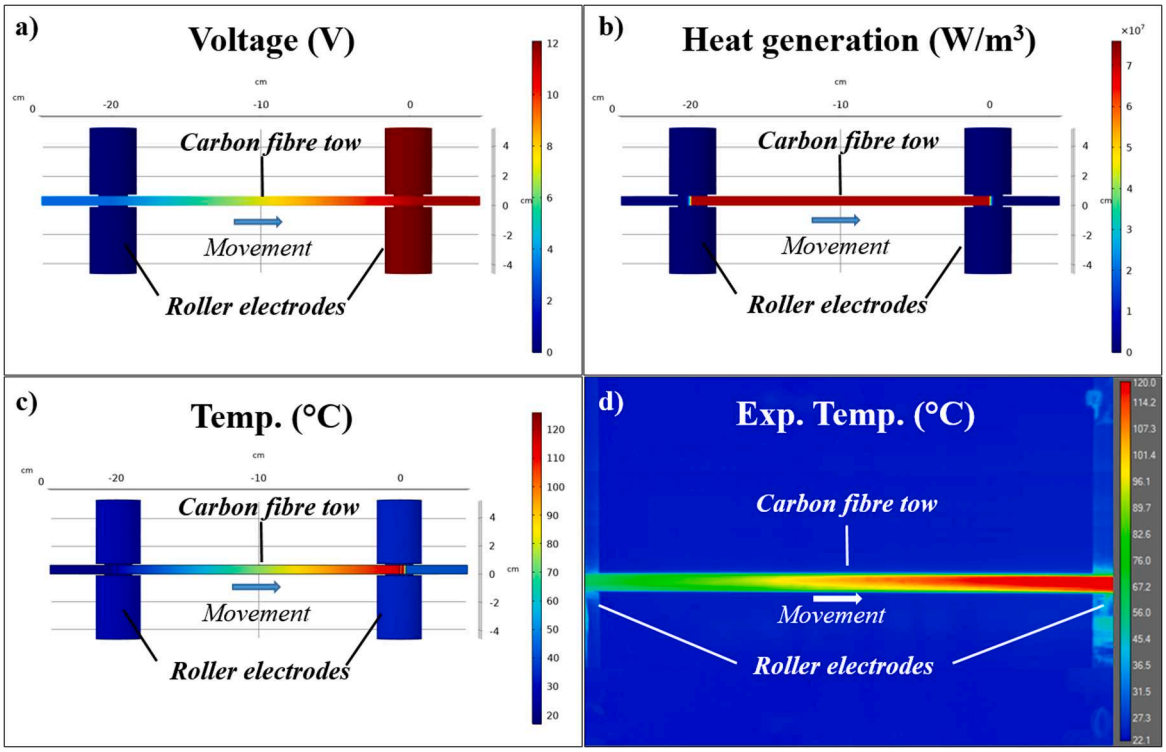

Fig. 4. Model predictions for **(a)** voltage **(b)** heat generation and **(c)** temperature distribution. **(d)** Thermal camera experimental image of the carbon fibre tow. (For interpretation of the references to colour in this figure legend, the reader is referred to the web version of this article.)

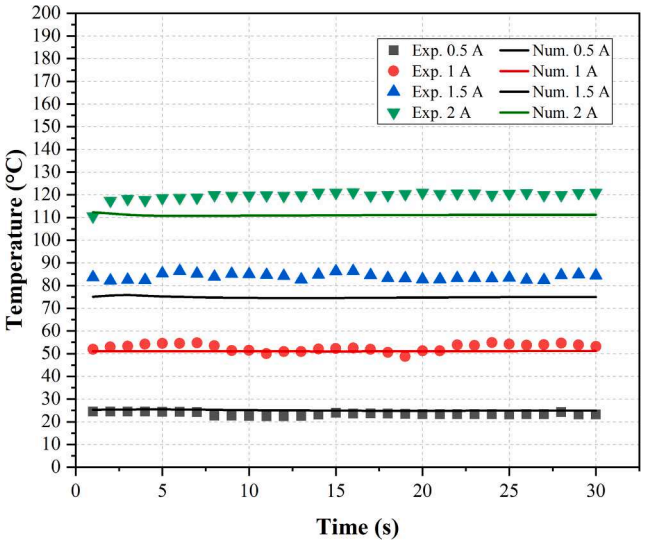

Fig. 5. Comparison of experimental maximum temperatures with model predictions at different currents. Note that experimental temperatures are the average of the temperatures measured across the tow width at the point of maximum temperature. (For interpretation of the references to colour in this figure legend, the reader is referred to the web version of this article.)

maximum temperature region is under 8 % in the processing window of towpreg, where the target temperature is around 120 °C.

A typical thermal camera image is given in Fig. 6, as well as surface plot of temperatures across the width at the hottest section of the tow. At a given time, tension can change momentarily across the width of the tow, due to a number of different factors, such as fibre packing, roller friction or a small lag during the unwinding from the spool. As explained earlier, the local variations of electrical resistance lead to high and low temperature regions as shown in Fig. 6a. Generally, high temperature regions are near the centre of the tow, while the sides have a lower temperature (Fig. 6b). Nevertheless, depending on the tension profile, high temperature regions can be observed at different places. The difference between the maximum and minimum temperature across the width can be significant, which is the reason why the model results were compared against the average temperatures in Fig. 5. Localised high temperatures increase the average temperature, and as the model does not account for such tension difference across the width of the tow, the slight discrepancy between the model predictions and the experimental results was observed. Furthermore, the tow is inherently heterogeneous and the temperature profile might not be the same for all segments, along the length of the tow that is being heated. As a result of this, instantaneous random local temperature spikes were also observed in the tow (Fig. 7) when a constant current is supplied. These variations are smaller when the average temperature across the tow width is considered, rather than a single point on the tow. In order to validate the numerical models, constant current was supplied in the heating zone, however, during the actual towpreg production, a PID controller is used to adjust the power input based on temperature readings. The PID controller performs well in keeping the average temperature in a reasonable range for the towpreg production, by controlling the power input.

The model predictions of temperature along the tow in the heating zone and experimental measurements from the centre and side of the tow are shown in Fig. 8. A disparity was observed between the model and experimental temperatures of the centre and side of the carbon fibre tow. This deviation was attributed to the aforementioned uneven tension, and also to the fact that the model assumes a perfect thermal contact with the rollers (i.e. no thermal contact resistances), which results in more heat transfer to the rollers than in the experimental case. In terms of the towpregging production, the average temperature of the tow near the maximum temperature region is the critical temperature for the complete melt of the powder epoxy, and the model performs better for this temperature, as shown in Fig. 5. Many Joule heating

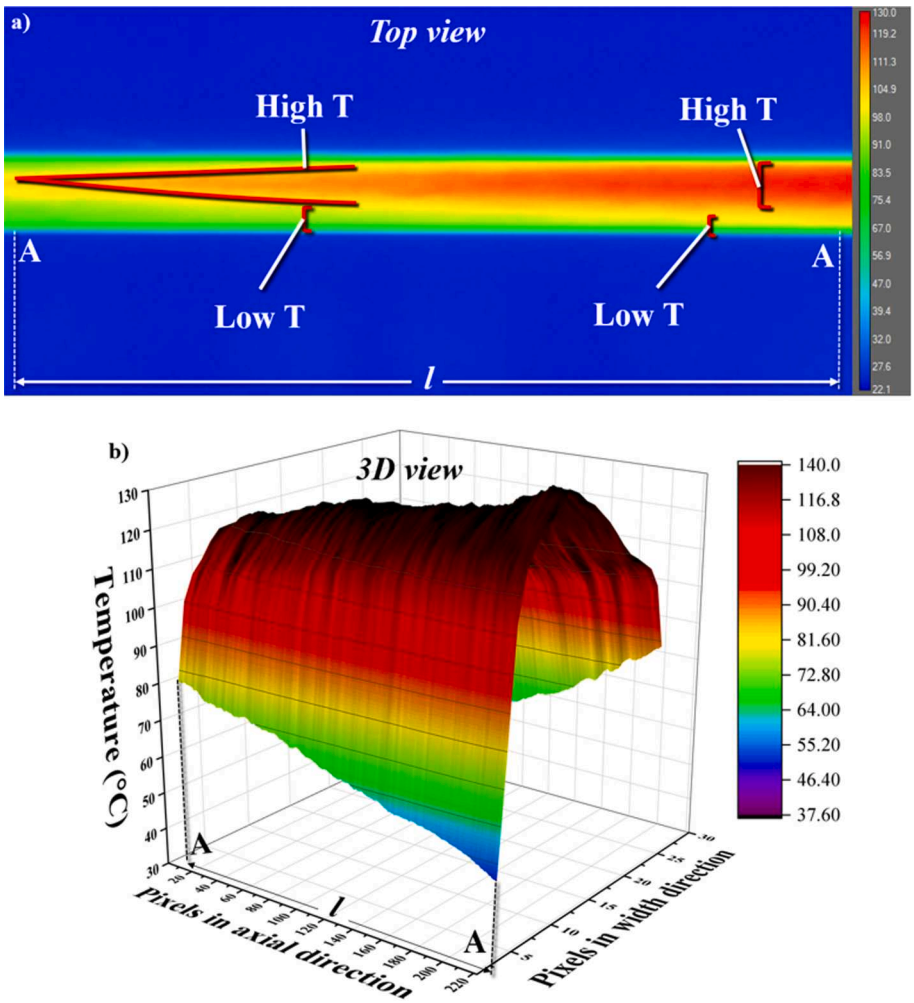

Fig. 6. **(a)** Experimental temperature variations across the width using an IR thermal camera (top view), a high temperature region near the top edge was formed. Note that rollers are out of field of view of the thermal camera. **(b)** Surface plot of the variations of temperature for the same area, captured by the IR thermal camera. (For interpretation of the references to colour in this figure legend, the reader is referred to the web version of this article.)

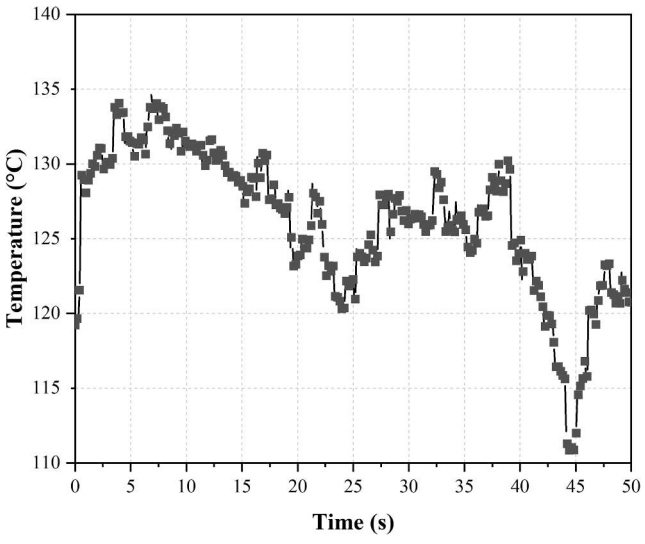

Fig. 7. Local temperature fluctuations over time for a selected point on the tow.

models have been documented in the literature to have similar inaccuracies, especially at higher temperatures or currents [27,33,37,38]. Up to 40 % higher predicted temperatures were presented by Chien et al. [37] for a Joule heating model for polyacrylonitrile/carbon nanotube composite fibres, which they explained by referring to inconsistency in fibre diameters, interfacial resistances between the nanotubes and polymer matrix, and altered material properties at high temperatures. Kwok and Hahn [33] reported a major discrepancy between their FEA model predictions and experimentally measured temperature values (>70 °C) due to the difference in actual and simulated resistivity values. Grohmann [38] presented a Joule heating model for a fibre placement application, which overpredicted the temperatures 30 % higher due to the actual material properties being different from what was used in the model.

One of the important phenomena observed in the Joule heating system of the tape is the effect of electrical contact resistances. Due to the imperfect contacts occurring between the carbon fibre tow and the copper rollers, electrical contact resistances occur and cause additional heating at the carbon fibre-roller surfaces. The influence of contact heating can be observed in the temperature distribution captured by the thermal camera. Normally, in the heating section, one can expect a temperature gradient that begins from room temperature near the beginning of the heated section (first roller electrode) and reaches the maximum temperature near the second roller electrode. However, as shown in Fig. 4d, the average temperature of the carbon fibre tow is

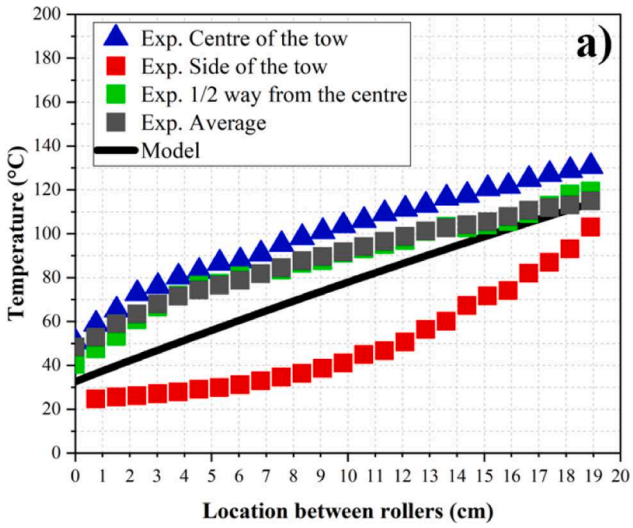

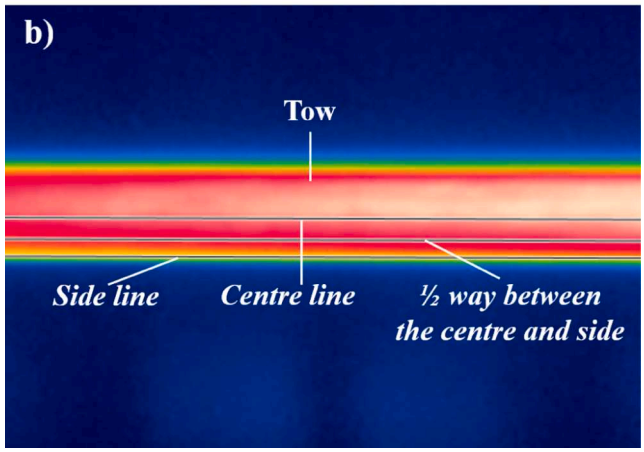

Fig. 8. **(a)** Comparison of model predictions of temperature along the tow with experimental temperatures from the centre and the side of the tow, **(b)** temperature measuring locations. (For interpretation of the references to colour in this figure legend, the reader is referred to the web version of this article.)

around 50 °C when it enters the heating zone, indicating that the heating actually starts as soon as the carbon fibre tow contacts the roller electrodes, due to the contact resistance heating (CRH) [45]. As previously mentioned, electrical contact resistances were accounted for in the model by creating an equivalent resistant thin film. Electrical contact resistance values for the corresponding operational conditions were determined experimentally. By accounting for contact resistance heating, a similar trend was observed in the modelling results, where the carbon fibre tow enters the heating zone already heated (Fig. 4c and d). Likewise, the temperature of the roller electrodes was also increased, as the heat generated by the contact resistance heating diffuses through both the carbon fibre tow and the rollers. Interestingly, the presence of contact resistance might be beneficial in terms of powder melt, due to the heating of the first roller electrode and a resulting higher entrance region temperature of the tow. Fig. 9 illustrates the influence of CRH on the temperature of the tow, when plotted against the distance between the rollers. When the model calculates the temperature field for 25 % higher contact resistance heating, by defining a 25 % more resistant thin film (1.77 S/m conductivity), the agreement between the model and experimental results at the beginning of the heating zone improves. For 50 % higher contact resistance heating (1.18 S/m conductivity), the agreement improves further, pointing out the inaccuracy of neglecting thermal contact resistances in the model. It is highly likely that by

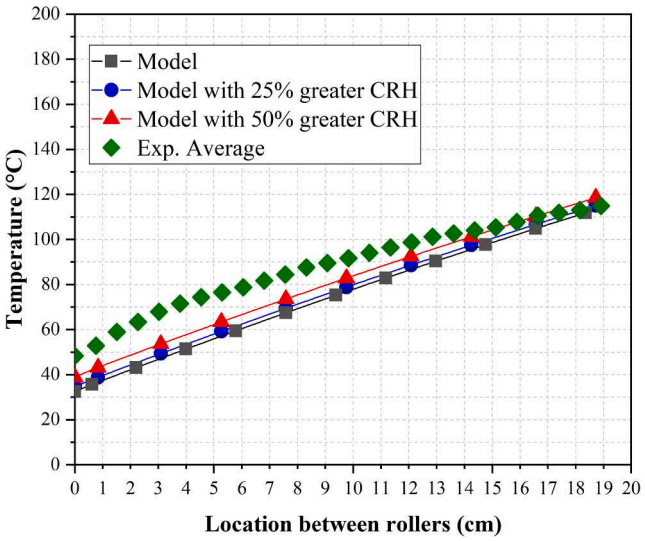

Fig. 9. Comparison of the experimental average temperature of the tow in the heating zone against the model results with different contact resistance heating (CRH) values. (For interpretation of the references to colour in this figure legend, the reader is referred to the web version of this article.)

assuming a perfect thermal contact between the rollers and the carbon fibre tow in the model, heat transfer to the rollers is overestimated, leading to a lower predicted temperature in the entry region.

4.2. Parametric studies of the model on the effect of operating parameters on the temperature distribution

While the aim of the presented towpreg production is to have a greater production rate with consistent quality, operating conditions have a substantial effect on the towpreg characteristics. For instance, higher production speeds mean that the carbon fibre tows spend less time in the powder deposition chamber, therefore, the amount of powder deposited changes with the production speed. Furthermore, the Joule heating time also reduces with high production speeds, consequently, for a given power input the maximum temperature reached is lower. Although powder epoxy has a relatively low melting temperature (~40 °C), higher operating temperatures are targeted in the heating section (~100–120 °C) to ensure the viscosity is minimal and good consolidation can be achieved without inducing significant cure. At high production speeds, these high temperatures may not be reached, so the power characteristics should be changed. The developed model was used to investigate the relationship between the production speed and the heating. Fig. 10 shows the modelled temperature change with respect to the production speed for the same power characteristics (2 A, constant current). The maximum temperature changes from 185 °C at 3 m/min to 64 °C at 15 m/min for the same power input. In order to attain a low viscosity at higher production speeds, the current supplied should be increased correspondingly, and possibly the power source should be replaced with a higher capacity-one.

Another alternative to reach targeted temperatures in the tapeline is to change the heating section length. This allows for a longer heating time for the tow, hence, the targeted temperature can be attained at lower power input. If the heating section length is too small, the maximum temperature on the tape might not be enough to fully melt the powder epoxy. It can be seen from model predictions in Fig. 11 that at the same current of 2 A, the maximum temperature of the tape changes remarkably with the electrode distance (i.e. heating section length). Considering the dimensions of the heating section, an electrode distance of around 20 cm was deemed to be optimal in order to maintain the targeted temperature (120 °C) for 2 A current.

As shown in Fig. 12a, the carbon fibre tow contacts the roller

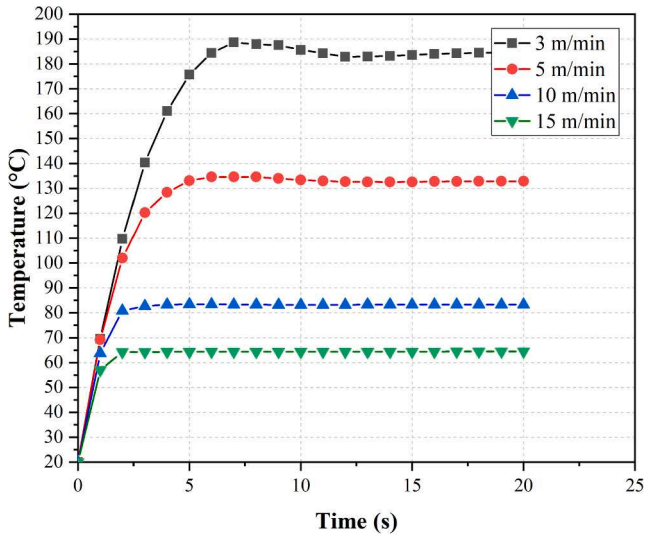

Fig. 10. Modelled change of maximum tow temperature with respect to different production speeds at 2 A of constant current. (For interpretation of the references to colour in this figure legend, the reader is referred to the web version of this article.)

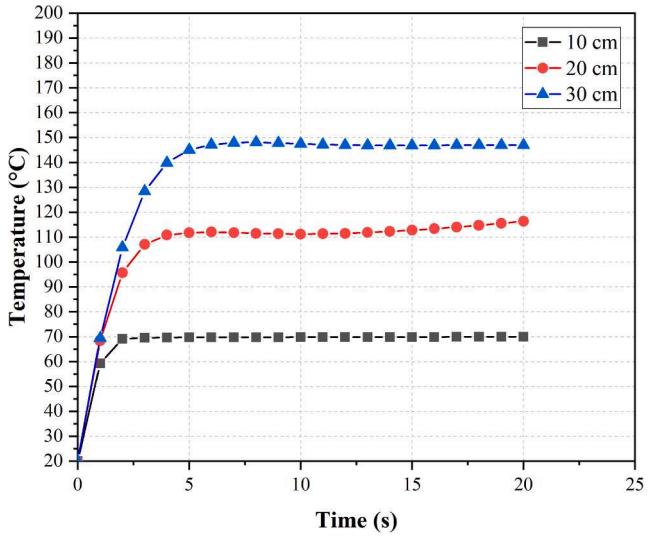

Fig. 11. Model predictions of the effect of electrode distance on the maximum temperature at 2 A current. (For interpretation of the references to colour in this figure legend, the reader is referred to the web version of this article.)

electrodes with an angle known as the wrap angle. Higher wrap angles increase the contact duration. Assuming the electrical contact resistances linearly increase with contact area, the influence of contact resistance heating is expected to be higher at greater wrap angles. Moreover, longer contact duration increases the conductive heat transfer between the carbon fibres and the roller electrodes. The model was used to evaluate the change in maximum temperature at different wrap angles. Fig. 12b compares the predicted temperatures for different wrap angles after 60 sec of production, where the initial temperature for the rollers and the tow is 20 °C. Since electrical contact resistances were not experimentally determined for different wrap angles, it was assumed that contact resistance values change linearly with the contact area. Kwok and Hahn's [33] measurements from wide and narrow silver paint electrodes revealed that electrical contact resistance values varied almost linearly with the contact area of the paint. With an increased wrap angle, hence greater contact area, the temperature at the entry region could be slightly increased even in a shorter production period

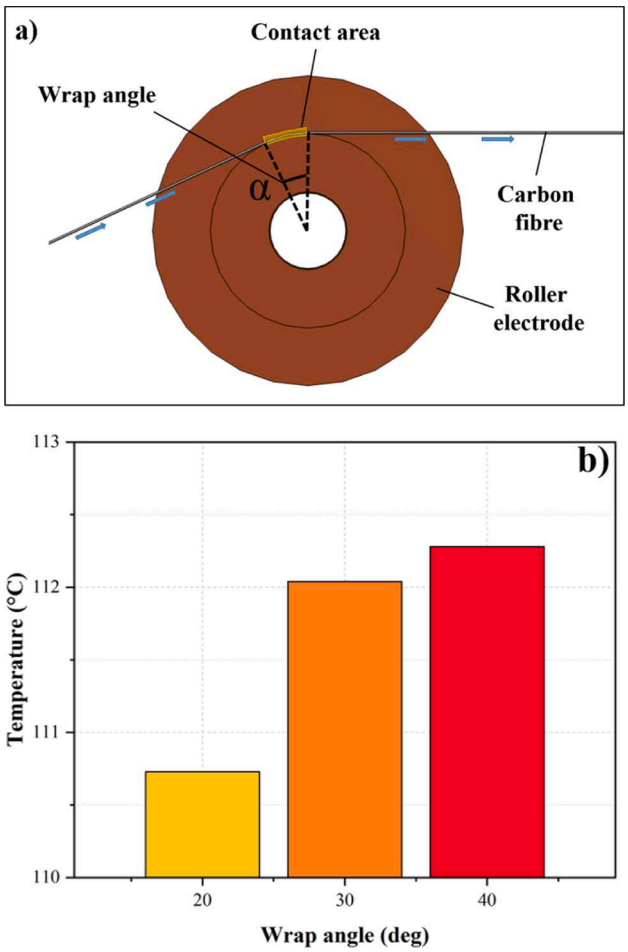

Fig. 12. **(a)** Wrap angle representation of the roller electrode, **(b)** model predictions of the maximum temperature reached after 60 s with respect to different wrap angles. (For interpretation of the references to colour in this figure legend, the reader is referred to the web version of this article.)

than 60 sec. As the roller temperature gradually increases due to the contact resistance heating in longer production runs, tow temperature can also further increase due to the increased conductive heat transfer from the rollers.

4.3. Melting behaviour of powder epoxy

It was demonstrated that the melting behaviour of polymer powders can be successfully characterised by using DSC data [43]. The melting of the powder epoxy in the tapeline was modelled by the semi-empirical melting equation Eq. (4) in COMSOL Multiphysics 5.6, where the coefficient and parameters of the equation were obtained by fitting the DSC data by Maguire [56]. The model results showed a good performance in describing the phase change of the powder epoxy as shown in Fig. 13, which compares the model predictions to the degree of melt captured by DSC scans by Maguire [56].

The melting model was coupled to the heat transfer model in order to predict when the melting of the powder epoxy occurs. The degree of melt, characterised by Eq. (4), is 0 when the powder epoxy is in solid form, and 1.0 when it is fully melted. It is important to melt all the powder epoxy as soon as it enters the heating section, in order to achieve low viscosity values in the tapeline. The complete melting of the powder epoxy can be compromised, particularly at high production speeds, which would lead to incomplete infiltration of resin into the carbon fibre tows. The melting model can be used to predict the location at which the melting is achieved, and also the optimal power configuration to provide

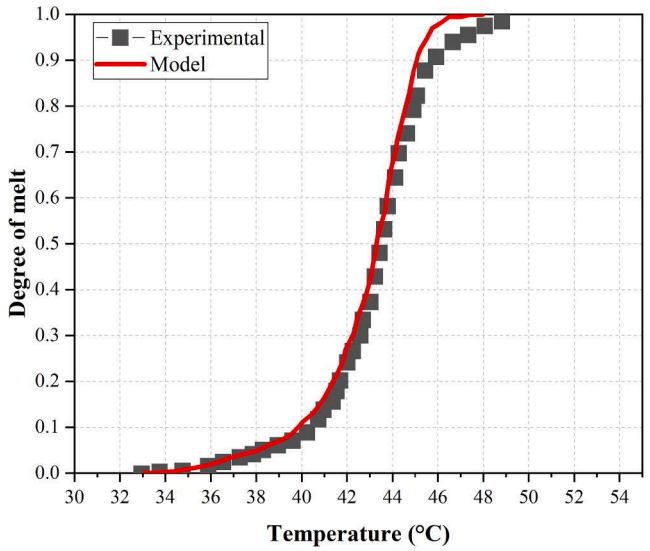

Fig. 13. COMSOL melting model predictions compared with experimental results converted from DSC data. (For interpretation of the references to colour in this figure legend, the reader is referred to the web version of this article.)

heating. As shown in Fig. 14b, powder epoxy is predicted to fully melt in the first 3 cm of the heating section, for the given operation conditions (2 A current, 20 N tension, and 6.5 m/min speed). Similar to Section 4.2., a parametric sweep can be carried out in the model in order to determine the maximum production speed that can provide melting in the heated section.

Increasing the temperature of powder epoxy above the melting point causes the viscosity of the molten polymer to decrease. The viscosity of the molten epoxy dictates how the powder particles sinter together and also the consolidation behaviour of the towpreg. Lower viscosity values cause molten powder epoxy to flow inside the carbon fibre easily, without external pressure. It was demonstrated [57] that the processibility of the powder epoxy is ideal at ~120 °C when the viscosity is low (~1 Pa·s) but the curing rate is slow at this temperature. Typically, the operational temperature in the tapeline is kept under 120 °C to avoid curing and burning additional components (sizing, pigments, fillers etc.) due to momentary surges and overshoots in temperature. Viscosity data for the powder epoxy presented in [57] was used in the model to check whether the viscosity is predicted to reach ideal conditions in the heating section (Fig. 15). The model shows that slower production speeds such as 3 m/min (hence, higher temperatures as discussed in Fig. 10) will allow the resin to reach a minimum viscosity, but the viscosity will begin to increase as the temperature exceeds 160 °C and significant curing will be induced. In contrast, for the given power characteristics, the model shows that higher production speeds (>10 m/min) will not be capable of reducing viscosity to an acceptable value for processing in the heating section. To ensure full sintering of the powder epoxy and a good consolidation by reaching an ideal viscosity, it is apparent that operating parameters should be adjusted as discussed in section 4.2.

4.4. Sintering of the powder epoxy

The sintering process in the tapeline is a complex phenomenon, which includes inherently stochastic parameters such as powder distribution or instantaneous fibre packing of the carbon fibre tows. Sintering results in a more homogenous impregnation, even without an external consolidation pressure. Visual evidence of the sintering process is presented in Fig. 16. The melted and re-solidified (and partially sintered) powder epoxy on the tow is composed of randomly distributed particles, with different sizes and morphology (Fig. 16a). Further temperature

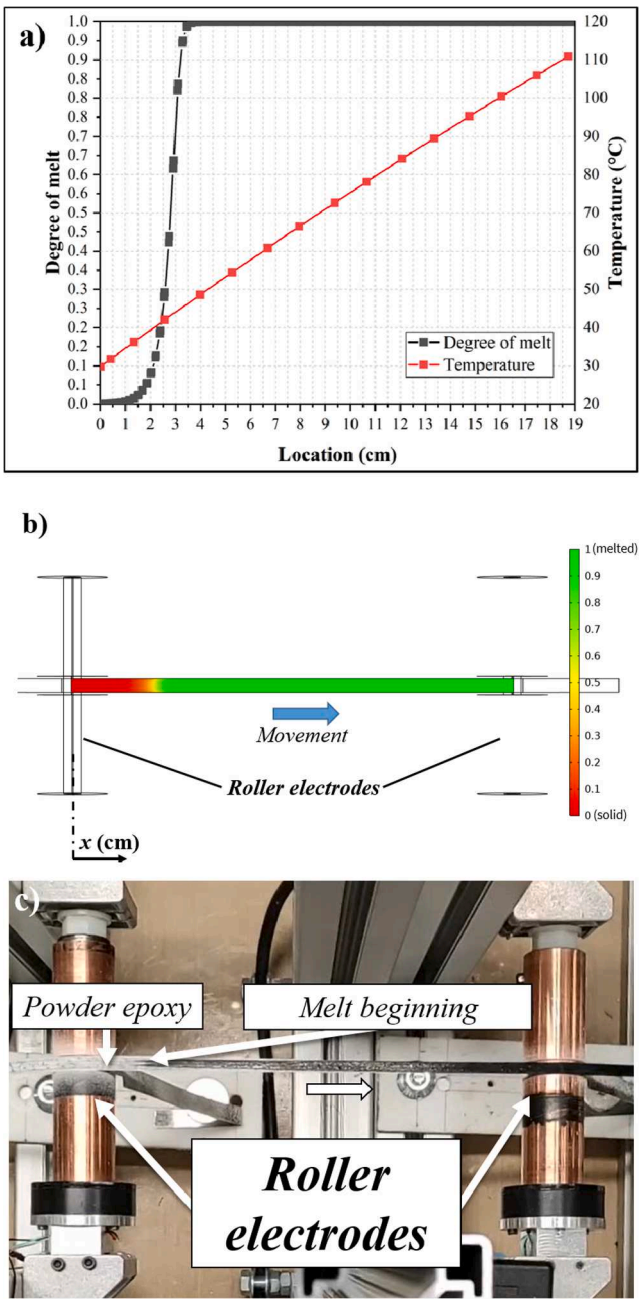

Fig. 14. (a) Model prediction of the degree of melt with respect to temperature for the given production run; (b) the degree of melt contours predicted by the model; (c) experimental image showing the melting of the powder. (For interpretation of the references to colour in this figure legend, the reader is referred to the web version of this article.)

increases beyond the point of sintering will result in viscosity reduction, followed by coalescence of individual melted powder epoxy sites, creating a uniform and homogenous, void-free layer (Fig. 16b).

For the sintering model characterised by Eq. (5), it was assumed that powder epoxy particles do not flow into the carbon fibre tow while sintering is taking place. Likely, sintering and the beginning of the resin flow happen concurrently, therefore a consolidation model that can describe the resin flow within the tow is required to fully understand the relationship between the sintering and the resin flow. This is out of the scope of this study, however, and Eq. (5) was only used as a simple check to determine if the temperatures reached in the tapeline are enough to sinter the powder epoxy. In situ experimental determination of the degree of sintering in the tapeline is difficult, because of this reason,

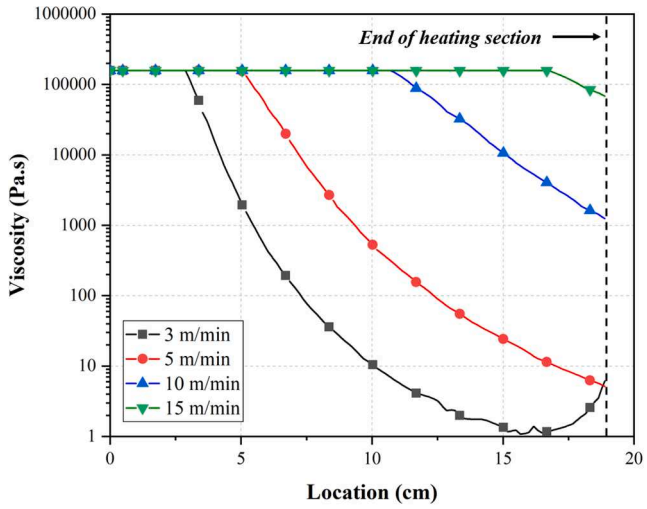

Fig. 15. Predicted viscosity values along the heating section at different production speeds. (For interpretation of the references to colour in this figure legend, the reader is referred to the web version of this article.)

experimental PPR data presented by Maguire et al. [23] was used to validate the sintering model. The model results showed a good performance in describing the sintering behaviour of the powder epoxy (Fig. 17), and it was coupled to the heat transfer model to analyse sintering during the production in the tapeline.

Sintering is characterised by the thickness change of the polymer bed, which is caused by powder compaction and bubble removal from the interfaces. Eq. (5) predicts the sintering ratio by providing the degree powder void fraction, at a given temperature and time interval. Opposite to the degree of melting parameter, fully sintered powder has a degree of sintering value of $\chi = 0$. For the initial sintering state of the powder epoxy, a powder void fraction value of 0.5 was assumed [23]. As a time and temperature-dependent process, sintering in the tapeline also exhibits a similar trend to temperature and melting behaviour. Model predictions reveal that at lower production speeds, 3 and 5 m/min, the powder epoxy on the carbon fibre completely sinters before leaving the heating section (Fig. 18a). This result is in line with the viscosity predictions, low viscosities achieved at low production speeds escalate the mobility of molten resin, and powder is completely sintered even in the short time (<10 s) it spends in the heating section. For the higher production speeds, although the powder is completely melted, the powder void fraction at the end of the heating section is 0.15 and 0.38 for 10 and 15 m/min, respectively. These results emphasise the requirement for higher input power at high production speeds. Fig. 18b illustrates the model predictions for higher currents at 15 m/min production speed. These results show that it is possible to sinter the powder completely at high production speeds by increasing the supplied power slightly.

5. Conclusions

This study demonstrates the analysis capabilities of modelling tools for a powder-epoxy based tapeline. The tapeline aims to produce high-quality, low cost towpregs for AFP applications. The Joule heating system in the line provides an efficient heating system with very low power consumption. An FEA model of the Joule heating system was developed to analyse heating characteristics in detail. The model predictions matched well with the thermal camera captures of the heating process, although small discrepancies were observed due to the temperature variations across the width of the carbon fibre tow, which were caused by tension inhomogeneity. It was shown that contact resistance heating (CRH) has a significant effect on the tow temperature at the beginning of the heating zone (entry region). Process parameters, such as power input, production speed, heating section dimensions and electrode geometry, were analysed in detail using the model to determine their effects on the heating system. The heat transfer model was coupled to semi-empirical melting and sintering models to determine optimum conditions for the towpreg production. Results suggest that by carefully adjusting input power and heating section geometry, desired temperatures can be reached in the system. Lower production speeds were found to be ideal for more controlled, consistent production runs. As higher production speeds are targeted in the tapeline (in order to increase

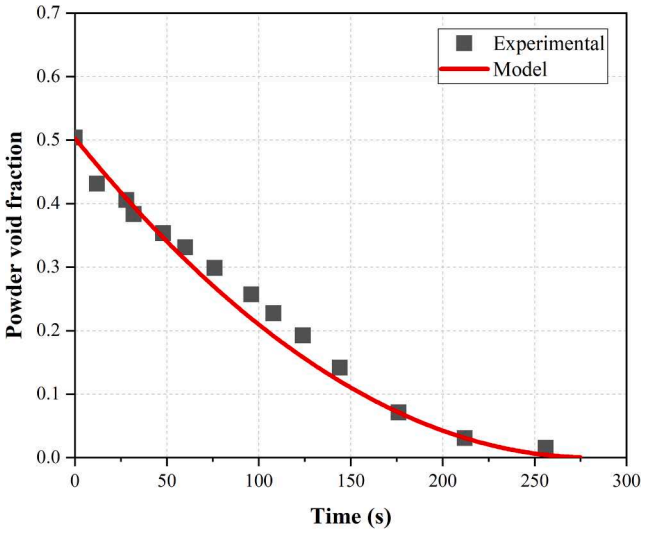

Fig. 17. Comparison of sintering model predictions with PPR test data given in [23]. (For interpretation of the references to colour in this figure legend, the reader is referred to the web version of this article.)

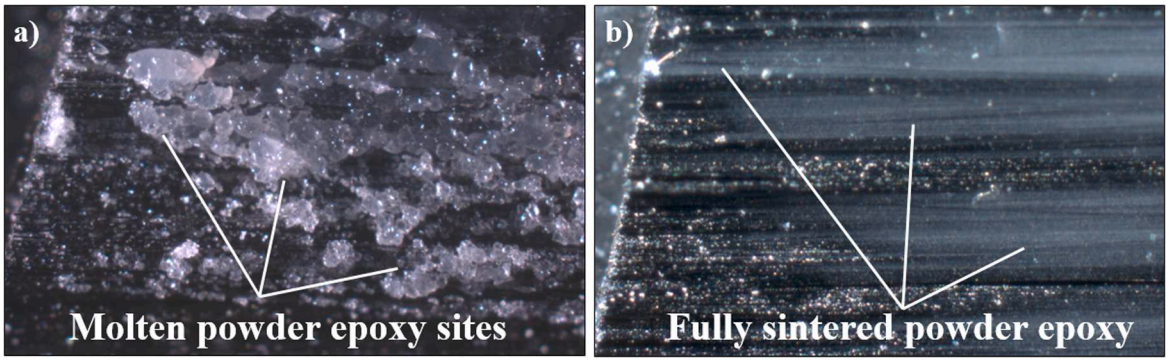

Fig. 16. Sintering process on the towpreg with time and temperature increase. (For interpretation of the references to colour in this figure legend, the reader is referred to the web version of this article.)

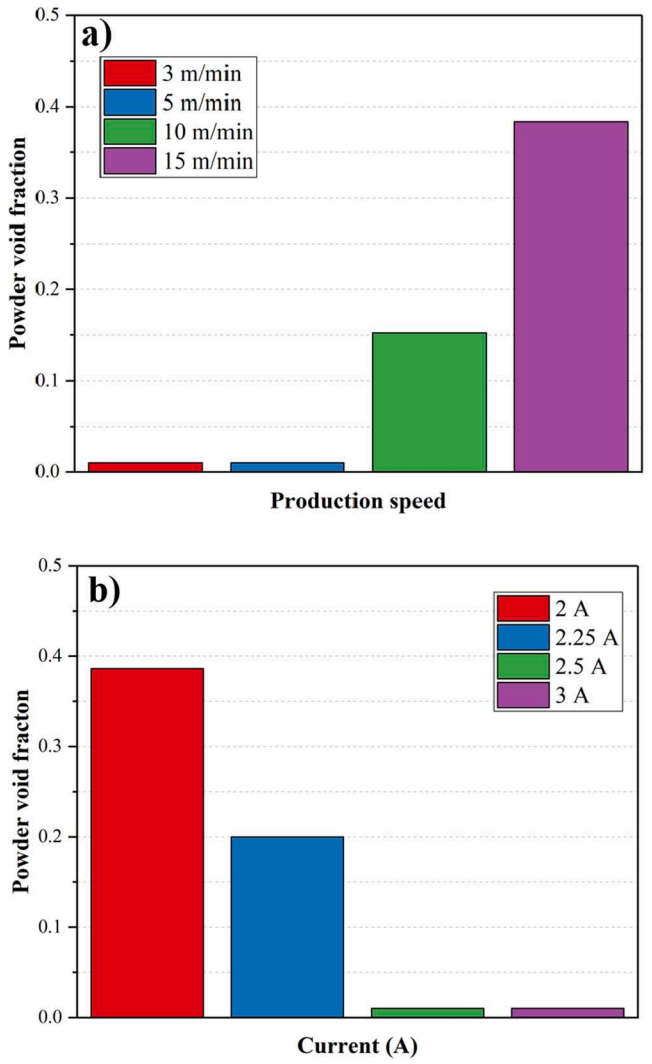

Fig. 18. Model predictions for minimum degree of powder void fraction reached at **(a)** different production speeds and **(b)** different currents at 15 m/min production speed. (For interpretation of the references to colour in this figure legend, the reader is referred to the web version of this article.)

production rate and thereby reduce cost), it was demonstrated that a more powerful power source would be needed. Melting and sintering models revealed that complete sintering might not be achieved at higher line speeds with the current setup, despite the powder epoxy being fully melted.

Due to the complex nature of the sintering process and its relationship with the consolidation flow, further resin flow models are required. A consolidation model that is coupled to the presented heat transfer model would allow analysing the possible concurrent sintering and resin flow into the carbon fibre tow. Investigating the resin distribution within the carbon fibre tow is crucial to improve the system design for improving the towpreg quality, which is recommended for future work.

CRediT authorship contribution statement

Murat Çelik: Conceptualization, Methodology, Software, Validation, Formal analysis, Investigation, Data curation, Writing – original draft, Visualization. **James M. Maguire:** Conceptualization, Methodology, Formal analysis, Software, Writing – review & editing. **Thomas Noble:** Validation, Investigation, Formal analysis, Writing – review & editing, Visualization, Data curation. **Colin Robert:** Conceptualization, Methodology, Resources, Writing – review & editing, Supervision, Project administration. **Conchúr M. Ó Brádaigh:** Conceptualization, Methodology, Resources, Writing – review & editing, Supervision, Project administration, Funding acquisition.

Declaration of Competing Interest

The authors declare that they have no known competing financial interests or personal relationships that could have appeared to influence the work reported in this paper.

Data availability

Data will be made available on request.

Acknowledgements

This study was part-funded by the UK EPSRC CIMCOMP Future Composites Manufacturing Research Hub (EP/P006701/1). The first author wishes to express his thanks for the financial support of the Republic of Turkey Ministry of National Education Scholarship Program.

References

[1] Grimshaw MN, Grant CG, Diaz JML. Advanced technology tape laying for affordable manufacturing of large composite structures. In: Int SAMPE Symp Exhib, vol 46 II, no 4; 2001. p. 2484–94.
[2] Oromiehie E, Prusty BG, Compston P, Rajan G. Automated fibre placement based composite structures: review on the defects, impacts and inspections techniques. Compos Struct 2019;224:110987.
[3] Brasington A, Sacco C, Halbritter J, Wehbe R, Harik R. Automated fiber placement: a review of history, current technologies, and future paths forward. Compos Part C Open Access 2021;6:100182.
[4] MarketsandMarkets, Global Prepreg Market by Type of Reinforcement (Carbon Fiber Prepreg, Glass Fiber Prepreg), Resin Type (Thermoset Prepreg, Thermoplastic Prepreg), Form, Manufacturing Process (Hot-melt, Solvent Dip), Application, and Region – Forecast to 2025. Marketresearch.com, USA; 2021. Accessed: Oct., 24, 2022. <https://www.marketresearch.com/MarketsandMarkets-v3719/Prepreg-Type-Reinforcement-Carbon-Fiber-14311752/>.
[5] Diao H, Robinson P, Wisnom MR, Bismarck A. Unidirectional carbon fibre reinforced polyamide-12 composites with enhanced strain to tensile failure by introducing fibre waviness. Compos Part A Appl Sci Manuf 2016;87:186–93.
[6] Esfandiari P, Silva JF, Novo PJ, Nunes JP, Marques AT. Production and processing of pre-impregnated thermoplastic tapes by pultrusion and compression moulding. J Compos Mater 2022;56(11):1667–76.
[7] Forcellese A, Mancia T, Russo AC, Simoncini M, Vita A. Robotic automated fiber placement of carbon fiber towpregs. Mater Manuf Process 2022;37(5):539–47.
[8] Arquier R, Iliopoulos I, Régnier G, Miquelard-Garnier G. Consolidation of continuous-carbon-fiber-reinforced PAEK composites: a review. Mater Today Commun 2022;32:104036.
[9] Van De Steene W, Verstockt J, Degrieck J, Ragaert K, Cardon L. An evaluation of three different techniques for melt impregnation of glass fiber bundles with polyamide 12. Polym Eng Sci 2018;58(4):601–8.
[10] McGregor OPL, Duhovic M, Somashekar AA, Bhattacharyya D. Pre-impregnated natural fibre-thermoplastic composite tape manufacture using a novel process. Compos Part A Appl Sci Manuf 2017;101:59–71.
[11] Wang S, Liu Y, Chen K, Xue P, Lin X, Jia M. Thermal and mechanical properties of the continuous glass fibers reinforced PVC composites prepared by the wet powder impregnation technology. J Polym Res 2020;27(4):1–12.
[12] Ho KKC, Shamsuddin S-R, Riaz S, Lamorinere S, Tran MQ, Javaid A, et al. Wet impregnation as route to unidirectional carbon fibre reinforced thermoplastic composites manufacturing. Plast Rubber Compos 2011;40(2):100–7.
[13] Asensio M, Esfandiari P, Núnez K, Silva JF, Marques A, Merino JC, et al. Processing of pre-impregnated thermoplastic towpreg reinforced by continuous glass fibre and recycled PET by pultrusion. Compos Part B Eng 2020;200:108365.
[14] Goud V, Alagirusamy R, Das A, Kalyanasundaram D. Influence of various forms of polypropylene matrix (fiber, powder and film states) on the flexural strength of carbon-polypropylene composites. Compos Part B Eng 2019;166:56–64.
[15] Goud V, Alagirusamy R, Das A, Kalyanasundaram D. Dry electrostatic spray coated towpregs for thermoplastic composites. Fibers Polym 2018;19(2):364–74.
[16] Goud V, Ramasamy A, Das A, Kalyanasundaram D. Box-Behnken technique based multi-parametric optimization of electrostatic spray coating in the manufacturing of thermoplastic composites. Mater Manuf Process 2019;34(14):1638–45.
[17] Khan AN, Alagirusamy R, Mahajan P, Das A. Multi-parametric investigation on the properties of powder-coated UHMWPE /LDPE towpreg manufactured through wet-electrostatic technique. Powder Technol 2022;401:117352.
[18] Khan AN, Goud V, Alagirusamy R, Mahajan P, Das A. Optimization study on wet electrostatic powder coating process to manufacture UHMWPE/LDPE towpregs. J Ind Text 2022;51:6686S–704S.

[19] Bowman S, Jiang Q, Memon H, Qiu Y, Liu W, Wei Y. Effects of styrene-acrylic sizing on the mechanical properties of carbon fiber thermoplastic towpregs and their composites. Molecules 2018;23(3):pp.
[20] Nunes JP, Siva JF. Production of thermoplastic matrix towpregs for highly demanding and cost-effective commercial applications. Mater Sci Forum 2013; 730–732:1030–5.
[21] Robert C, Pecur T, Maguire JM, Lafferty AD, McCarthy ED, Ó Brádaigh CM. A novel powder-epoxy towpregging line for wind and tidal turbine blades. Compos Part B Eng 2020;203:108443.
[22] Çelik M, Noble T, Jorge F, Jian R, Ó Brádaigh CM, Robert C. Influence of line processing parameters on properties of carbon fibre epoxy towpreg. J Compos Sci 2022;6(3):75.
[23] Maguire JM, Simacek P, Advani SG, Ó Brádaigh CM. Novel epoxy powder for manufacturing thick-section composite parts under vacuum-bag-only conditions. Part I: Through-thickness process modelling. Compos Part A Appl Sci Manuf 2020; 136:105969.
[24] Joseph C, Viney C. Electrical resistance curing of carbon-fibre/epoxy composites. Compos Sci Technol 2000;60(2):315–9.
[25] Sierakowski RL, Telitchev IY, Zhupanska OI. On the impact response of electrified carbon fiber polymer matrix composites: effects of electric current intensity and duration. Compos Sci Technol Mar. 2008;68(3–4):639–49.
[26] Zantout AE, Zhupanska OI. On the electrical resistance of carbon fiber polymer matrix composites. Compos Part A Appl Sci Manuf 2010;41(11):1719–27.
[27] Athanasopoulos N, Koutsoukis G, Vlachos D, Kostopoulos V. Temperature uniformity analysis and development of open lightweight composite molds using carbon fibers as heating elements. Compos Part B Eng 2013;50:279–89.
[28] Xu X, Zhang Y, Jiang J, Wang H, Zhao X, Li Q, et al. In-situ curing of glass fiber reinforced polymer composites via resistive heating of carbon nanotube films. Compos Sci Technol 2017;149:20–7.
[29] Hayes SA, Lafferty AD, Altinkurt G, Wilson PR, Collinson M, Duchene P. Direct electrical cure of carbon fiber composites. Adv Manuf Polym Compos Sci 2015;1 (2):112–9.
[30] Joo SJ, Yu MH, Kim WS, Kim HS. Damage detection and self-healing of carbon fiber polypropylene (CFPP)/carbon nanotube (CNT) nano-composite via addressable conducting network. Compos Sci Technol 2018;167:62–70.
[31] Orellana J, Moreno-Villoslada I, Bose RK, Picchioni F, Flores ME, Araya-hermosilla R. Self-healing polymer nanocomposite materials by joule effect. Polymers 2021;13(4):1–24.
[32] Mas B, Fernández-Blázquez JP, Duval J, Bunyan H, Vilatela JJ. Thermoset curing through Joule heating of nanocarbons for composite manufacture, repair and soldering. Carbon N Y 2013;63:523–9.
[33] Kwok N, Hahn HT. Resistance heating for self-healing composites. J Compos Mater 2007;41(13):1635–54.
[34] Zanjani JSM, Saner Okan B, Pappas PN, Galiotis C, Menceloglu YZ, Yildiz M. Tailoring viscoelastic response, self-heating and deicing properties of carbon-fiber reinforced epoxy composites by graphene modification. Compos. Part A Appl. Sci. Manuf. 2018;106:1–10.
[35] Athanasopoulos N, Sikoutris D, Panidis T, Kostopoulos V. Numerical investigation and experimental verification of the Joule heating effect of polyacrylonitrile-based carbon fiber tows under high vacuum conditions. J Compos Mater 2012;46(18): 2153–65.
[36] Athanasopoulos N, Kostopoulos V. Resistive heating of multidirectional and unidirectional dry carbon fibre preforms. Compos Sci Technol 2012;72(11): 1273–82.
[37] Chien AT, Cho S, Joshi Y, Kumar S. Electrical conductivity and Joule heating of polyacrylonitrile/carbon nanotube composite fibers. Polymer (Guildf) 2014;55 (26):6896–905.
[38] Grohmann Y. Continuous resistance heating technology for high-speed carbon fibre placement processes. SAMPE Europe 2020;2020:3–12.
[39] Lu M, Xu J, Arias-Monje PJ, Gulgunje PV, Gupta K, Shirolkar N, et al. Continuous stabilization of polyacrylonitrile (PAN) - carbon nanotube (CNT) fibers by Joule heating. Chem Eng Sci 2021;236:116495.
[40] Kontopoulou M, Vlachopoulos J. Melting and densification of thermoplastic powders. Polym Eng Sci 2001;41, no. 2 SPEC. ISS:155–69.
[41] Bellehumeur CT, Tiang JS. Simulation of non-isothermal melt densification of polyethylene in rotational molding. Polym Eng Sci 2002;42(1):215–29.
[42] Bellehumeur CT, Bisaria MK, Vlachopoulos J. An experimental study and model assessment of polymer sintering. Polym Eng Sci 1996;36(17):2198–207.
[43] Greco A, Maffezzoli A. Polymer melting and polymer powder sintering by thermal analysis. J Therm Anal Calorim 2003;72(3):1167–74.
[44] Kandis M, Bergman TL. Observation, prediction, and correlation of geometric shape evolution induced by non-isothermal sintering of polymer powder. J Heat Transfer 1997;119(4):824–31.
[45] Çelik M, Noble T, Haseeb A, Maguire JM, Robert C, Ó Brádaigh CM. Contact resistance heating of unidirectional carbon fibre tows in a powder-epoxy towpregging line. Plast Rubber Compos 2022;51(8):383–92.
[46] Sandberg M, Yuksel O, Baran I, Spangenberg J, Hattel JH. Steady-state modelling and analysis of process-induced stress and deformation in thermoset pultrusion processes. Compos Part B Eng 2021;216:108812.
[47] Volk M, Wong J, Arreguin S, Ermanni P. Pultrusion of large thermoplastic composite profiles up to Ø 40 mm from glass-fibre/PET commingled yarns. Compos Part B Eng 2021;227:109339.
[48] Minchenkov K, Vedernikov A, Kuzminova Y, Gusev S, Sulimov A, Gulyaev A, et al. Effects of the quality of pre-consolidated materials on the mechanical properties and morphology of thermoplastic pultruded flat laminates. Compos Commun 2022; 35:101281.
[49] Trende A, Åström BT, Wöginger A, Mayer C, Neitzel M. Modelling of heat transfer in thermoplastic composites manufacturing: double-belt press lamination. Compos Part A Appl Sci Manuf 1999;30(8):935–43.
[50] Deng K, Zhang C, Dong X, Fu KK. Rapid and energy-efficient manufacturing of thermoset prepreg via localized in-plane thermal assist (LITA) technique. Compos Part A Appl Sci Manuf 2022;161:107121.
[51] Shi B, Shang Y, Zhang P, Cuadros AP, Qu J, Sun B, et al. Dynamic capillary-driven additive manufacturing of continuous carbon fiber composite. Matter 2020;2(6): 1594–604.
[52] Vashisth A, Healey RE, Pospisil MJ, Oh JH, Green MJ. Continuous processing of pre-pregs using radio frequency heating. Compos Sci Technol 2020;195:108211.
[53] Toray, "Toray T700S Standard Modulus Carbon Fiber."; 2018. p. 2.
[54] COMSOL AB, "COMSOL Multiphysics® v. 5.6." Stockholm, Sweden.
[55] Jeon EB, Fujimura T, Takahashi K, Kim HS. An investigation of contact resistance between carbon fiber/epoxy composite laminate and printed silver electrode for damage monitoring. Compos Part A Appl Sci Manuf 2014;66:193–200.
[56] Maguire JM. Processing of thick section epoxy powder composite structures. The University of Edinburgh; 2019. PhD dissertation.
[57] Maguire JM, Nayak K, Ó Brádaigh CM. Characterisation of epoxy powders for processing thick-section composite structures. Mater Des 2018;139:112–21.